

# RAIN RATE RETRIEVAL USING THE 183-WSL ALGORITHM

Sante Laviola<sup>1</sup> and Vincenzo Levizzani<sup>1</sup>

<sup>1</sup> National Research Council – Institute of Atmospheric Sciences and Climate, Bologna, Italy

## 1. INTRODUCTION

One of the main open scientific challenges lasting since a few decades is the compelling need for a substantial improvement of techniques adopted to retrieve precipitation intensities and their duration in time. This is particularly pressing for those precipitation episodes that interest very small areas, where also light rains are often trigger disastrous flooding events. Note that an accurate knowledge of the terrain features such as morphological and orographic aspects is crucial.

In this context, satellite sensors with their large number of spectral bands and their wide spatial coverage can be easily employed for a global research and monitoring strategy. In particular, the increasing spatial resolutions of the new passive microwave (PMW) sensors and the constantly increasing number of orbiting platforms are providing data at an unprecedented temporal frequency.

Usually, PMW estimation algorithms for the retrieval of rain rates or of other atmospheric parameters (e.g., Grody et al. 2000, Ferraro et al. 2005) are based on two different approaches: scattering and absorption. Scattering methods infer rain intensities by exploiting the brightness temperature depression due to the frozen hydrometeors located in the upper part of the cloud. The scattering signal (or index) is strictly linked to the probability of melting ice crystals into the clouds and their conversion into rain droplets. As demonstrated by Bennartz et al. (2002) the measure of the

scattering signature can be efficiently used to select and classify rain rate intensities distinguishing conditions ranging from no-rain to heavy rain. The quantitative comparison with co-located radar data shows the robustness of the technique in classifying heavier precipitation characteristic of a convective system, where the amount of scatterers is relatively large.

The second approach is founded on the water vapor properties to absorb and successively emit the radiation centered on specific absorption bands (Grody 1991, Staelin et al. 1999, 2000). As to this method, the retrieval at low and high frequencies must be considered differently. If the retrieval is carried out at low frequencies, i.e. around the water vapor band at 22.235 GHz, the scattering is weak and the absorption dominates the extinction. Nevertheless, Wang et al. (1989) note that this absorption band provides only enough sensitivity to measure the total column water vapor and the high emissivity background masks the atmospheric contribution over land. On the other hand, at higher frequencies the scattering effect increases also into the strong absorption bands such as at 183.31 GHz. The presence of cold clouds can depress the brightness temperature particularly for the frequencies located farther from the center of the absorption line (Greenwald et al. 2002, Burns et al. 1997).

In this work, we report the results of two new fast algorithms over land and ocean to estimate rain rates using PMW opaque frequencies of the Advanced Microwave Sounding Unit module B (AMSU-B) of the National Oceanic and Atmospheric Administration (NOAA). Our choice of using these frequencies is mainly founded on considerations reported in section 2 and other studies not reported here. In section 3

---

*Corresponding author address:* Sante Laviola, CNR-ISAC, via Gobetti 101, I-40129 Bologna, Italy, e-mail: s.laviola@isac.cnr.it

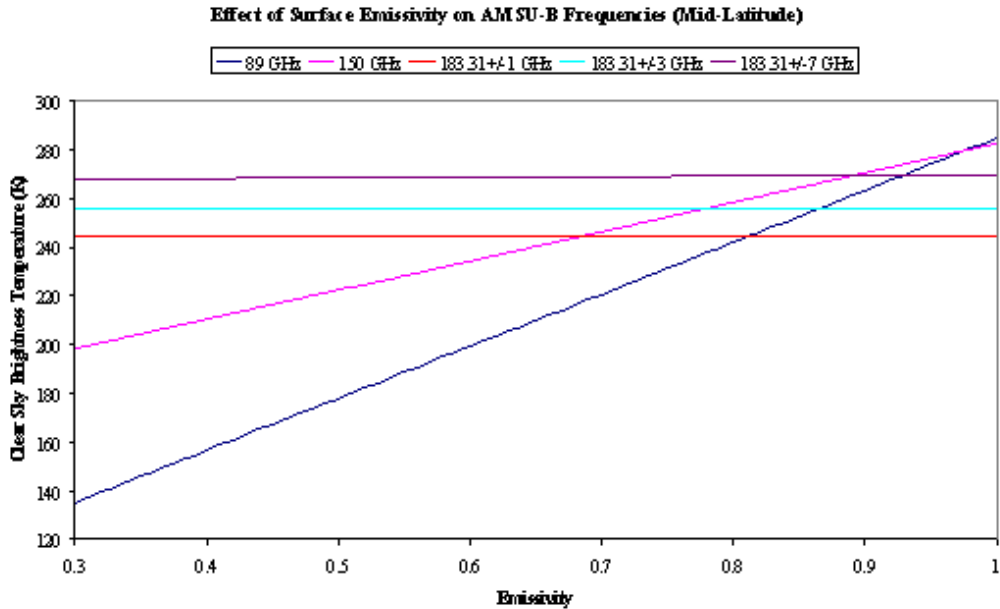


FIGURE 1. Emissivity effects on the AMSU-B channels. The two window channels are strongly dependent on the surface emissivity showing an increasing value up to 280 K from the simulated sea surface ( $\epsilon = 0.50$ ) to dry land ( $\epsilon = 1.00$ ). At moisture frequencies, where the weighting functions are higher than window, the surface emissivity effect is low.

a few case studies are presented where the new algorithm at 183 GHz (called hereafter 183-WSL) is compared with a precipitation index (hereafter called MSG-PI) initially proposed for AVHRR by Thoss et al. (2001) but here modified to fit the channels of Meteosat Second Generation (MSG) Spinning Enhanced Visible and InfraRed Imager (SEVIRI, Schmetz et al. 2002). In the same section, we discuss the method for validating the precipitation type classification by comparing the 183-WSL results ( $\text{mm h}^{-1}$ ) with the co-located Scattering Index (SI) values.

## 2. 183.31 GHZ SENSITIVITY TO SURFACE EMISSIVITY AND RAINY CLOUD ALTITUDES

Since the 183.31 GHz bands are mainly dedicated to the sounding of the atmospheric water vapor amount (Kakar 1983, Wang et al. 1989), several studies have demonstrated the effects of clouds on these frequencies and their possible application into retrieval schemes. Note

that the use of PMW information is necessary to detect rainy systems or correct and integrate infrared (IR) measurements, for instance in the blended techniques. However, their use is limited because of the variability of surface emissivity ( $\epsilon$ ). Grody et al. (2000) proposed a few algorithms based on different land type studies to evaluate surface emissivity using AMSU data.

Here we chose radiative transfer results with different values of surface emissivity, which refers to land if  $\epsilon$  is typically  $> 0.6$  and to water in the other cases, to quantify the effect of surface on AMSU-B channels.

Figure 1 shows the simulated brightness temperatures for all AMSU-B frequencies as a function of surface emissivity in clear sky conditions. The results are obtained by a adding/doubling radiative transfer model (Evans et al., 1995a,b) running with mid-latitude profiles and coupled to Rosenkranz (2001) for the computation of the absorption at selected frequencies.

As we can expected, the signal around 89 and 150 GHz has strong surface contributions showing a deep depression near low emissivity values and converging

about to same brightness temperature when  $\epsilon=1$  (dry-land). Therefore, the decreasing surface emissivity from dry-land value to water bodies enhances the influence of atmospheric moisture on these channels. Another significant aspects of Fig. 1 is that, since their weighting functions are peaked beyond 2 km altitude, the three moisture channels are little or not affected by different emissivities thus suggesting their application both over land and over sea.

Other sensitivity studies not reported here have emphasized that, when moving towards higher latitudes where the atmosphere is less optically thick, the contribution of surface emissivity affects more and more the measurement

particularly at 190 GHz where also thinner ice clouds can modify then signal.

Precipitating cloud altitude is another important variable affecting the AMSU-B brightness temperatures. We studied the behavior of AMSU-B moisture channels as a function of the position of a rainy cloud in the troposphere. All simulations have been carried out using radiosonde temperature and humidity profiles screening out the possible cloud formations along balloon trajectory with the threshold suggested by Karstens et al. (1994). The cloud structure is built adopting a Marshall-Palmer's water drop size distribution (Marshall et al. 1948) and the Mie theory to solve the scattering equations.

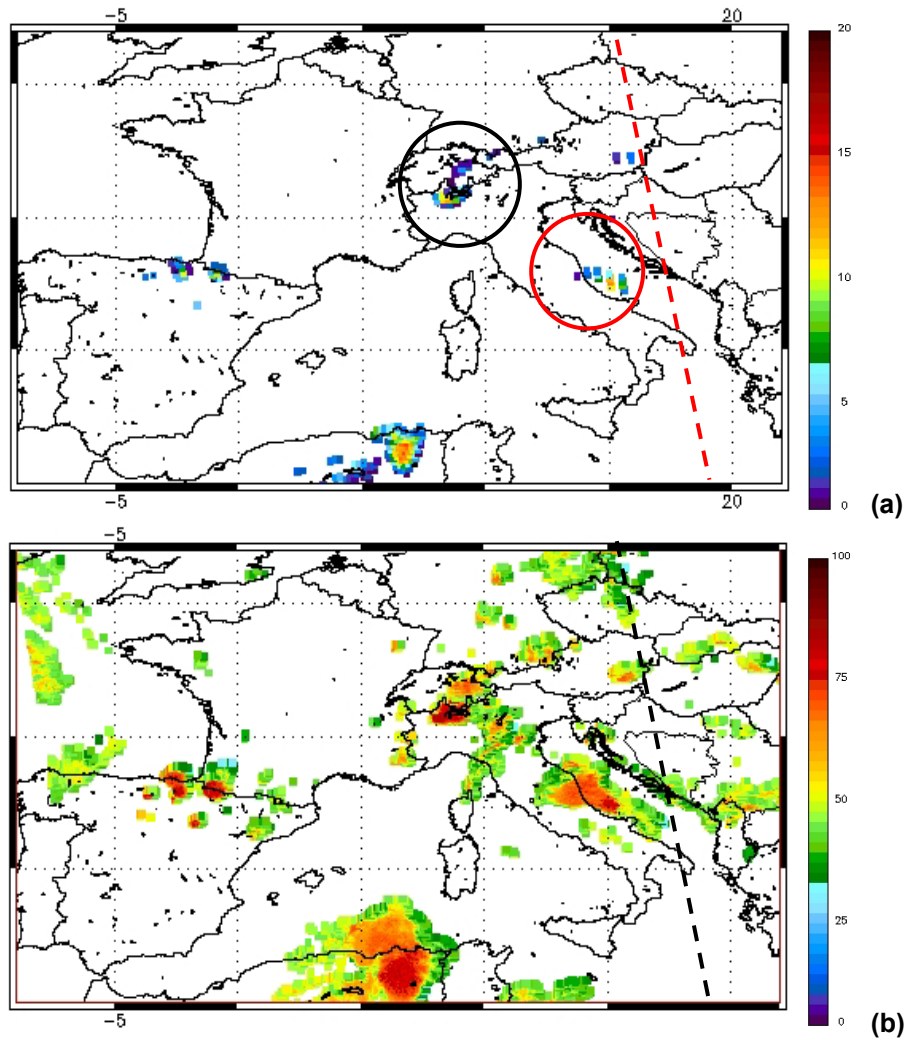


FIGURE.2. 12 June 2007, 2112 UTC: a) 183-WSL; b) MSG-PI. Dashed lines delimit the edge of the AMSU-B swath.

In agreement with the weighting function distribution, our results show that only rainy clouds positioned above 2 km altitude interact with opaque frequencies at 183.31 GHz and the interaction will be always more intense as the cloud becomes thicker.

### 3. METHOD AND APPLICATIONS

In the following a method to discriminate and possibly classify precipitation type is presented. Our classification scheme is based on a series of thresholds suitable for removing water vapor contributions from the 183-WSL algorithm results and separate stratiform rain from convective.

As a comparison we have used the Bennartz et al. (2002) rain-intensity classes to check our classification and quantify the precipitation rates for each class.

Figure 2 and 4 depict two case studies related to a series of precipitating events affecting the Mediterranean area during June 2007. Note that the 183-WSL algorithm is successful in correctly discriminating precipitating from just scattering clouds.

Figure 2 shows three interesting aspects: 1) Mesoscale Convective System (MCS). In the lower part of the figure we can spot an MCS moving from the African coast towards the Mediterranean Sea. Needless to say that in this case the detection is rather easy

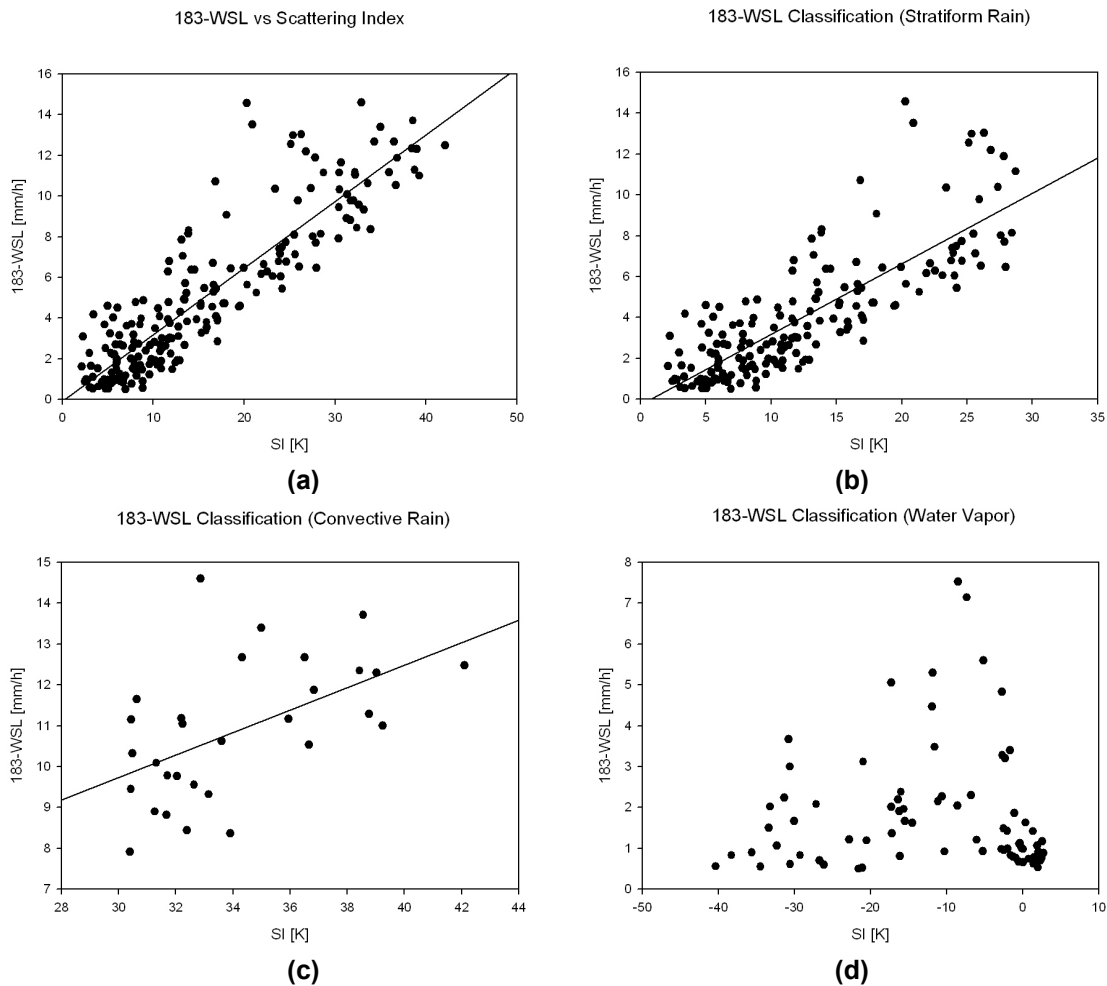


FIGURE 3. 12 of June 2007, 2112 UTC: a) scatter plot of 183-WSL vs SI; b) classification of stratiform rain compared to SI values; c) classification of convective rain compared to SI values; d) classification of water vapor values removed from the retrieval.

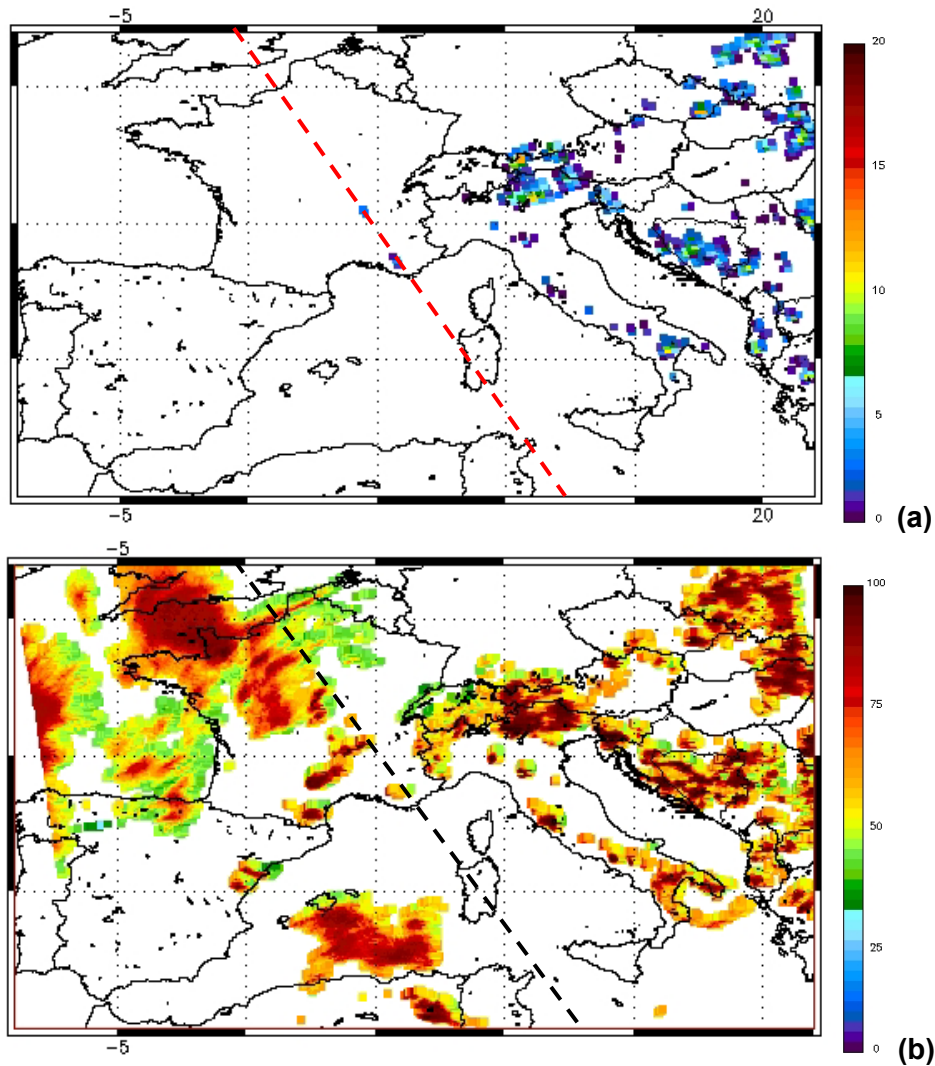


FIGURE 4. Same as in Fig. 2 but for 12 June 2007, 2112 UTC.

because during the formation of a deep convective system the greater amount of surrounding water vapor is condensed inside the cloud or strictly close to its border. Precipitation intensities associated to the different parts of the MSC can be distinguished moving from the convective core (red) to the cloud edge. Moreover, from the large rainy area detected in b) only higher scattering values ( $PI > 80$ ) are flagged as precipitating by the 183-WSL.

2) Coastal system (red circle). This system is not characterized by heavy precipitation but the water vapor around the clouds has been filtered out using a threshold embedded into the retrieval scheme.

3) Orographic system (black circle). A small orographic cloud system close to the Alps is detected even if we did not evaluate the effects of snow cover and surface roughness on the AMSU-B channel 5.

Figure 3 shows a quantitative summary of the method's classification thresholds. The scattergrams describe how the high correlation between the 183-WSL and the SI (4-a) is mainly due to the stratiform rain (4-b) instead of the convective portion (4-c). Many pixels where precipitation intensities are up to  $8 \text{ mm h}^{-1}$  (4-d) have been flagged as water vapor and then removed from the retrieval.

Particularly interesting is the situation reported in Fig. 4 where only stratiform rain

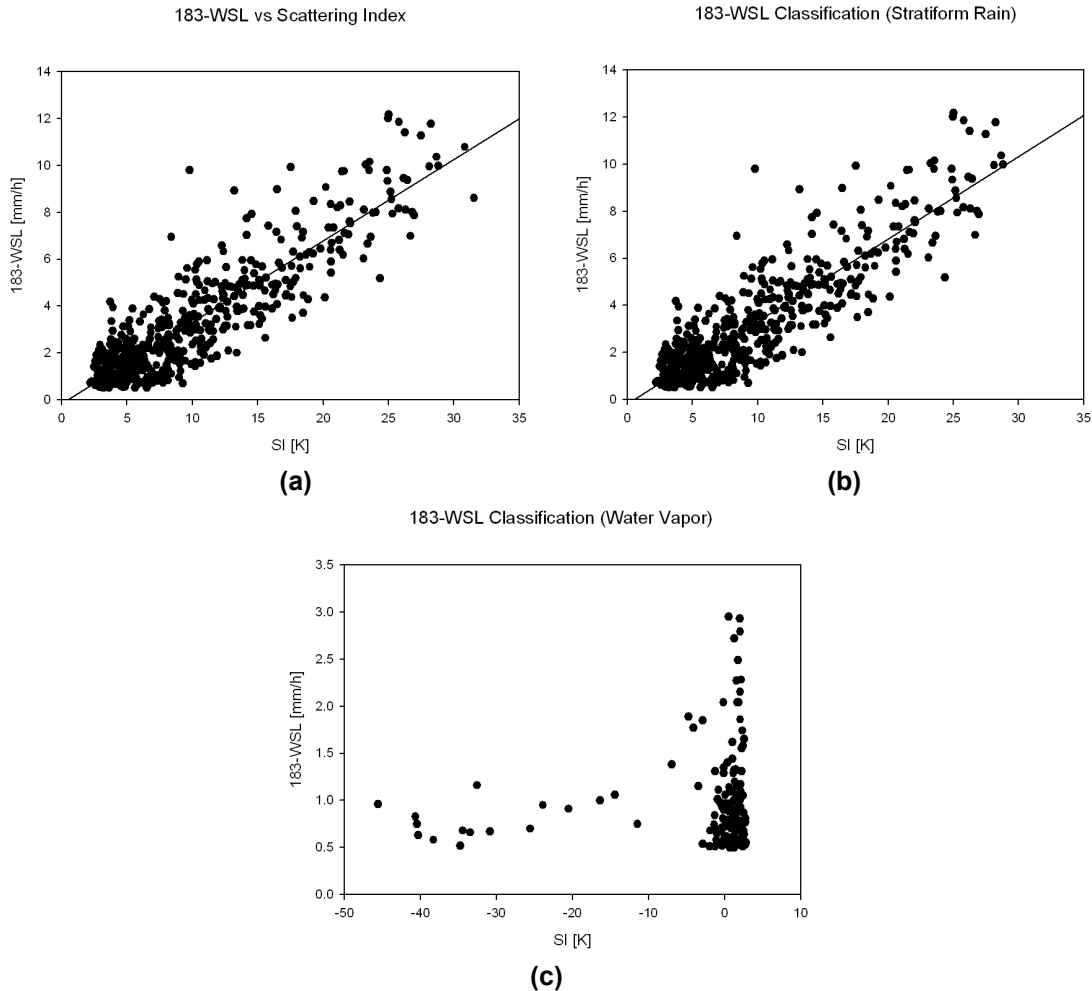


FIGURE 5. 12 of June 2007, 2112 UTC: a) scatter plot between 183-WSL vs SI; b) classification of stratiform rain compared to SI values; c) classification of water vapor values removed from the retrieval.

classification were selected. A fast comparison with the SI Fig. 5 shows that all precipitating pixels are classified as stratiform and water vapor. Figure 5-b and 5-c in particular show that low and very low precipitation intensities ( $< 3 \text{ mm h}^{-1}$ ) would be associated to the stratiform rain class if the water vapor threshold were not removed from the computations.

#### 4. CONCLUSIONS AND FUTURE WORK

Results of two new algorithms based on NOAA/AMSU-B 183.31 GHz absorption channels are presented. Although these frequencies are fully employed to retrieve

the atmospheric water vapor, we develop two equations suited for calculating rain rates both over land and over water surfaces.

The drawback of these algorithms is their direct link with the atmospheric water vapor amount when condensation clusters are formed both in cloud free regions and in the surroundings of rainy clouds but not directly involved in the precipitation process. Our studies have shown that absorption due to the water vapor contaminates the algorithm estimations labeling as rainy some pixels in which only water vapor absorption was detected.

In order to prevent these incorrect rain-flags we calculate a series of thresholds to

evaluate only water vapor contribution, to classify rain types and estimate precipitation intensities for each class. The results encourage us to apply the method to precipitation events characterized by different features for a better understanding of the algorithm performances and an improvement of rain delineation in the winter season and at latitudes higher than 60 degrees.

## BIBLIOGRAPHY

- Bennartz, R., and A. Thoss, 2002: Precipitation analysis using the Advanced Sounding Unit in support of nowcasting applications. *Meteorol. Appl.*, **9**, 177-189.
- Burns, B. A., X. Wu, and G. R. Diak, 1997: Effects of precipitation and clouds ice on brightness temperatures in AMSU moisture channels. *IEEE Trans. Geosci. Remote Sensing*, **35**, 1429-1437.
- Evans, F., and G. F. Stephens, 1995a: Microwave radiative transfer through clouds composed of realistically shaped ice crystal. Part I: single scattering properties. *J. Atmos. Sci.*, **52**, 2041-2057.
- Evans, F., and G. F. Stephens, 1995b: Microwave radiative transfer through clouds composed of realistically shaped ice crystal. Part II: single scattering properties. *J. Atmos. Sci.*, **52**, 2058-2072.
- Ferraro, R. R., F. Weng, N. C. Grody, L. Zhao, H. Meng, C. Kongoli, P. Pellegrino, S. Qiu, and C. Dean, 2005: NOAA operational hydrological products derived from the Advanced Microwave Sounding Unit. *IEEE Trans. Geosci. Remote Sensing*, **43**, 1036-1049.
- Greenwald, T. J., and S. A. Christopher S. A., 2002: Effect of cold clouds on satellite measurements near 183 GHz. *J. Geophys. Res.*, **107**, D13, AAC 3-1, AAC 3-6.
- Grody, N. C., 1991: Classification of snow cover and precipitation using the Special Sensor Microwave/Imager. *J. Geophys. Res.*, **96**, 7423-7435.
- Grody, N. C., F. Weng, and R. R. Ferraro R., 2000: Application of AMSU for obtaining hydrological parameters. In: *Microwave Radiometry and Remote Sensing of the Earth's Surface and Atmosphere*, P. Pampaloni and S. Paloscia, Eds., USP Int. Science Publishers, Utrecht, 339-352.
- Kakar, R. K., 1983: Retrieval of clear sky moisture profiles using the 183 GHz water vapor line. *J. Climate Appl. Meteor.*, **22**, 1282-1289.
- Karstens, U., C. Simmer, and E. Ruprecht, 1994: Remote sensing of cloud liquid water. *Meteor. Atmos. Phys.*, **54**, 157-171.
- Marshall, J. S., and W. McK. Palmer, 1948: The distribution of raindrops with size. *J. Meteor.*, **5**, 165-166.
- Marshall, J. S., R. C. Langille, and W. McK. Palmer, 1947: Measurement of rainfall by radar. *J. Meteor.*, **4**, 186-192.
- Rosenkranz, P. W., 2001: Retrieval of temperature of moisture profiles from AMSU- and AMSU-B measurements. *IEEE Trans. Geosci. Remote Sensing*, **39**, 2429-2435.
- Schmetz, J., P. Pili, S. Tjemkes, D. Just, J. Kerkmann, S. Rota, and A. Ratier, 2002: An introduction to Meteosat Second Generation (MSG). *Bull. Amer. Meteor. Soc.*, **83**, 977-992.
- Staelin, D. H., and F. W. Chen, 2000: Precipitation observations near 54 and 183 GHz using the NOAA-15 satellite. *Proc. 2000 IEEE Int. Geoscience and Remote Sensing Symp.*, **38**, 5, 2322-2332.
- Staelin, D. H., F. W. Chen, and A. Fuentes, 1999: Precipitation measurements using 183-GHz AMSU satellite observations. *Proc. 1999 IEEE Int. Geosci. and Remote Sensing Symp.*, **4**, 2069-2071.
- Thoss, A., A. Dybbroe, and R. Bennartz, 2001: The Nowcasting SAF precipitating clouds product. *Proc. 2001 EUMETSAT Satellite Data Users' Conf.*, Antalya, 1-5 Oct., 399-406.
- Wang, J. R., T. T. Wilheit, and L. A. Chang, 1989: Retrieval of total precipitable water using radiometric measurements near 92 and 183 GHz. *J. Appl. Meteor.*, **28**, 146-154.

## ACKNOWLEDGMENTS

Support from the Progetto Strategico della Regione Puglia "Nowcasting avanzato con l'uso di tecnologie GRIS e GIS" and from EUMETSAT's Satellite Application Facility in support to Hydrology and Operational Water Management are gratefully acknowledged. Discussions with F. J. Turk were very helpful.